Available online at www.sciencedirect.com
SCIENCE DIRECT®
Journal of Nuclear Materials 337–339 (2005) 196–200
journal of nuclear materials
www.elsevier.com/locate/jnucmat

Radiation belts in the Wendelstein-7AS stellarator

U. Wenzel *, H. Thomsen, Y. Feng, P. Grigull, K. McCormick

Max-Planck-Institut für Plasmaphysik, Euratom Association, D-17493 Greifswald, Germany

Abstract

At high plasma density we find two types of radiation belts at the edge of the Wendelstein-7AS stellarator. The first one is observed in the inboard scrape-off layer (SOL) when the edge plasma is detached. It seems to be specific to the stellarator. The second one is found on closed flux surfaces and resembles the Marfe phenomenon known from tokamaks. They are experimentally characterized and modeling calculations are presented.

PACS: 52.55.H; 52.40.H
Keywords: Divertor detachment; Marfe; H-alpha measurement; W7-AS

1. Introduction

The installation of the island divertor in the Wendelstein-7AS (W7-AS) stellarator allowed access to a new operation regime. In the high density H-mode (HDH) very high line-averaged densities (up to $4 \times 10^{20}\,\mathrm{m}^{-3}$) were quasi-stationary maintained over many tens energy confinement times [1]. In discharges close to the density limit the edge plasma cools down and the plasma radiation detaches from the divertor target plates [2]. Detachment was also detected by a drop of the ion saturation current and the H_α emission in the divertor plasma [3]. These features are very typical also for the detachment process in tokamaks [4]. In this article we describe another observation which seems to be specific for the stellarator edge plasma: the formation of a toroidal carbon radiation belt in the inboard scrape-off layer (SOL).

Radiation belts are also observed in tokamaks. They are the result of a radiative condensation phenomenon on closed flux surfaces (Marfe) [5]. Such kind of radiation belt occurs also in the stellarator W7-AS. As a consequence, the confined energy is degraded up to 50%. In this way Marfes form a density limit in the stellarator [6]. We characterize both types of radiation belts and discuss the physical mechanisms.

2. Experimental

Fig. 1 shows the time traces of discharge #54470. We distinguish two phases. The density is rapidly ramped-up so that the plasma is at the density limit in the first phase (from 0.2 to 0.45 s). In the second phase (from 0.55 to 0.8 s) the line-averaged density is a bit lower so that the plasma transits into a stable detached state. The magnetic configuration is the standard configuration (rotational transform $\iota_a = 5/9$), but with an enhanced plasma radius of 13.6 cm due to the appropriate control coil currents. The neutral beam

* Corresponding author. Tel.: +49 3834 88 2482; fax: +49 3834 88 2009.
E-mail address: uwe.wenzel@ipp.mpg.de (U. Wenzel).

0022-3115/$ - see front matter © 2004 Elsevier B.V. All rights reserved.
doi:10.1016/j.jnucmat.2004.09.030

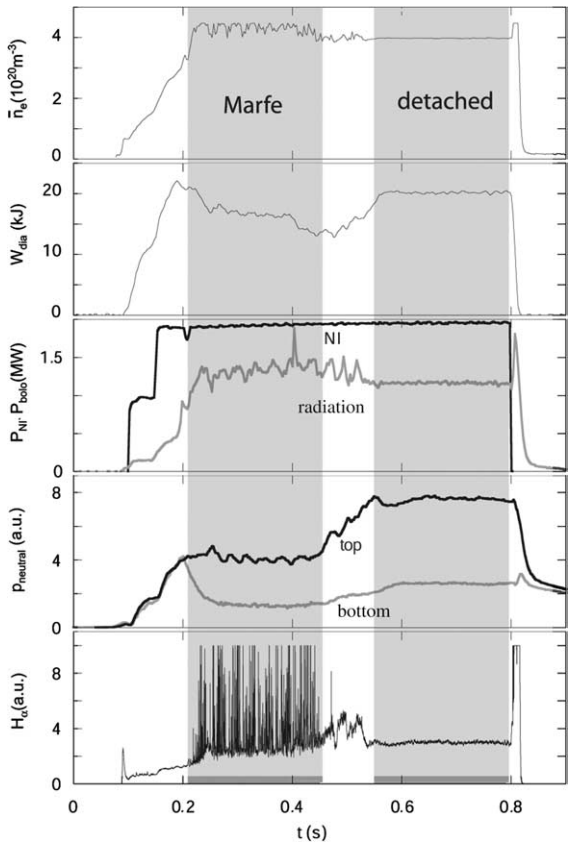

Fig. 1. Signal traces of the Wendelstein-7AS discharge #54470: line-averaged density from bremsstrahlung (n_e), energy content (W_{dia}), neutral beam (P_{NI}) and total radiated power (P_{bolo}), sub-divertor neutral pressures ($p_{neutral}$) and H_α-signal from midplane. The density is ramped-up to the density limit which is characterized by the Marfe. Afterwards the density is slightly reduced so that the plasma transits into the detached state.

power is 2MW (P_{NI}). In the first phase the confinement is degraded as evident by the drop in the diamagnetic energy (W_{dia}). The midplane H_α emission strongly oscillates which is also reflected in the total radiated power.

The sub-divertor neutral pressure in the lower divertor drops. In the second phase the sub-divertor neutral pressure from the lower divertor recovers but now the pressure on top increases. This is a typical feature of the detached plasma in W7-AS which is connected with strong volume recombination between the strike lines on top [7]. Since the direction of the asymmetry depends on the toroidal magnetic field we consider here only the standard case for W7-AS with a negative direction of the magnetic field. The density at the separatrix is about $4 \times 10^{19}\,\mathrm{m}^{-3}$ (midplane) and in the divertor $0.5 \times 10^{19}\,\mathrm{m}^{-3}$ [3].

The radiation in the plasma edge was investigated by a set of several CCD cameras. Fig. 6 shows the arrangement of the camera for the observation of the upper divertor. An equivalent camera was used for viewing the lower divertor. A picture of the bottom divertor is shown in Fig. 2. Both cameras were operated with different interference filters to sample the emission of hydrogen and the impurity ions. Since the lines-of-sight run through a large part of the plasma cross-section (cf. Fig. 6) the radiation from the plasma edge was also detected. In the following sections we study the distribution of the plasma radiation for the two characteristic discharge phases.

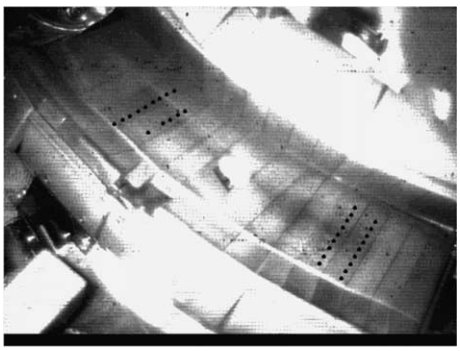

Fig. 2. Picture of the divertor module at bottom taken by a vertical viewing CCD camera. Target tiles 1 and 17 are respectively on the upper left and lower right corner of the image.

3. Plasma radiation in the detached phase

The detached plasma is characterized by a drop of the ion fluxes to the target plates. Since in some regions this drop is not prominent (the plasma stays attached) we have only a partial detachment.

Fig. 3 shows pictures of the divertor plasma at bottom taken with an H_α and a CIII ($\lambda = 465$ nm) interference filter. Data is from discharge #56244 at $t = 0.45$ s. The H_α picture shows the typical strike line pattern (two lines called B and D after [8]). In the CIII picture the corresponding strike lines are also visible. However, the most intense part of the radiation does not originate from the plasma target interaction but from the inboard SOL. The strike lines are only weakly pronounced. The radiation belt is absent or at least weak in the H_α emission. The stripe in the lower left corner of the CIII picture is an extension of the emission from the upper divertor module. Since the total radiative losses are mainly due to the carbon ions CIII and CIV we conclude that the main radiation in the detached state comes no longer from the divertor region but from the inboard edge plasma in the SOL.

Detailed numerical studies on detachment physics have been performed using the EMC3-EIRENE code

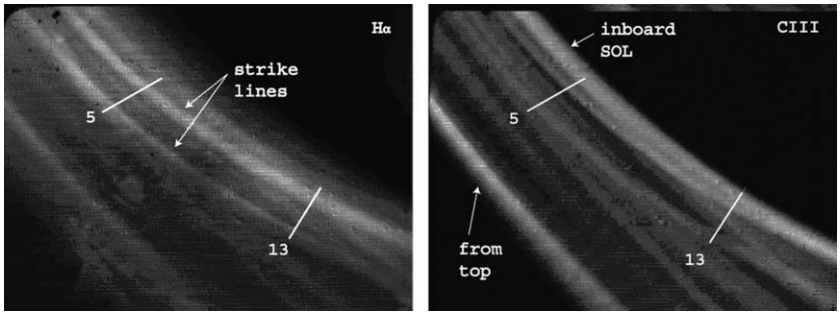

Fig. 3. View of the detached plasma in the lower divertor at bottom: H_α (left) and CIII (right). Data is from shot #56244 at $t = 0.45$ s. Target tiles 5 and 13 are indicated by white lines. The H_α picture shows two strike lines from the divertor. Contrary to this the CIII emission is dominated by a radiation belt from the inboard SOL; the carbon emission from the divertor strike lines is much weaker. The intense straight stripe in the left lower corner is an extension of a radiation zone from the upper divertor.

[9]. In detached plasmas the power balance in the island SOL is governed by carbon impurity radiation. In this case, the radiation level and location of the radiation zone are very sensitive to plasma parameters and island geometry. Fig. 4 shows the poloidal distribution of the total carbon radiation and the ionization source of hydrogen for the standard island divertor configuration ($\iota_a = 5/9$ with maximum control coil current). The plasma is partially detached (i.e. some parts at the target plates see a significant load of energy and particles). The carbon radiation layer is shifted from the target plates to the inboard SOL. Contrary to that the main ionization source is still in the divertor. The reason for the asymmetric carbon radiation is a corresponding asymmetry of the electron temperature. Due to the geometry of the flux surfaces the energy is preferentially fed into the outboard SOL. The poloidal temperature asymmetry explains why the divertor plate sections which are magnetically connected to the outboard SOL remain attached as observed in experiments [9]. Moreover, the inboard side location of the radiation layer keeps the divertor region sufficiently warm to prevent the recycling neutrals from penetrating into the core. In a good approximation the H_α emission is proportional to the ionization source (the ratio 'number of ionizations' to 'number of excitations' is approximately constant for hydrogen). Thus, the H_α emission is observed in the simulated divertor plasma in accordance with the experimental findings.

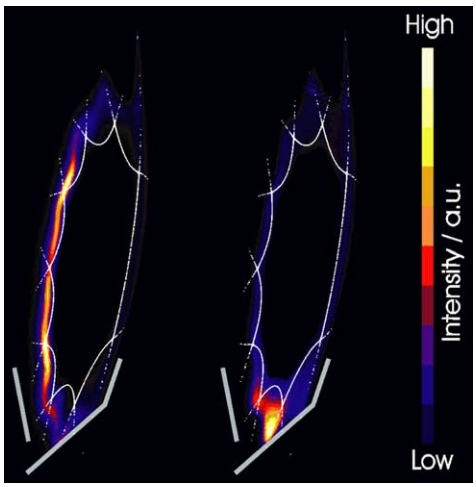

Fig. 4. Modeling results of a partially detached discharge: total carbon radiation (left) and ionization sources of hydrogen (right) (EMC3/Eirene code). The main radiation zone is shifted from the divertor to the inboard scrape-off layer. The temperature in the divertor is still sufficient to ionize the hydrogen atoms there.

4. Marfe formation

Increasing the density beyond the limit for stable partial detachment, we observe a radiation belt at the inboard side also in the H_α emission. Since its characteristics are very similar to those of Marfes observed in tokamaks [10] we will use this term here, too.

Fig. 5 shows the H_α emission in the upper divertor in the Marfe phase (#54470 at 0.4 s). It is very different from the typical strike line pattern (cf. Fig. 3). The inboard radiation is much more intense than the outer one. To intensify the faint outer strike line the intensity was cut at 0.04 W cm^{-2} resulting in a saturation of the inboard radiation. Furthermore, the inner radiation zone belt is oblique to the strike line (see the upper left corner of the picture). We conclude that the inner strike line is overlaid by a radiation belt which is prominent not only in the carbon radiation but also in the hydrogen emission.

The CCD cameras for divertor observation integrate the light over a complete plasma cross-section (Fig. 6). For the interpretation of the line-integrated images a

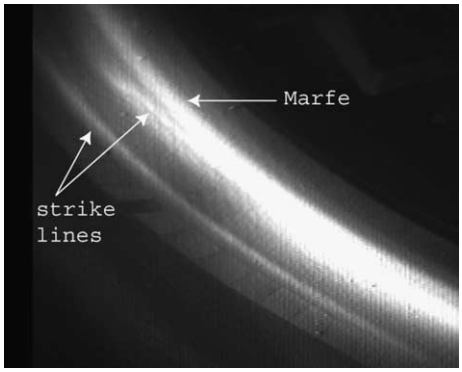

Fig. 5. H_α emission in the upper divertor from (#54470 at 0.4 s). The inner strike line is overlaid by an oblique radiation zone from the inboard plasma (Marfe). At tile number 1–4 the inner strike line is still visible. The view on the outer strike line is not influenced.

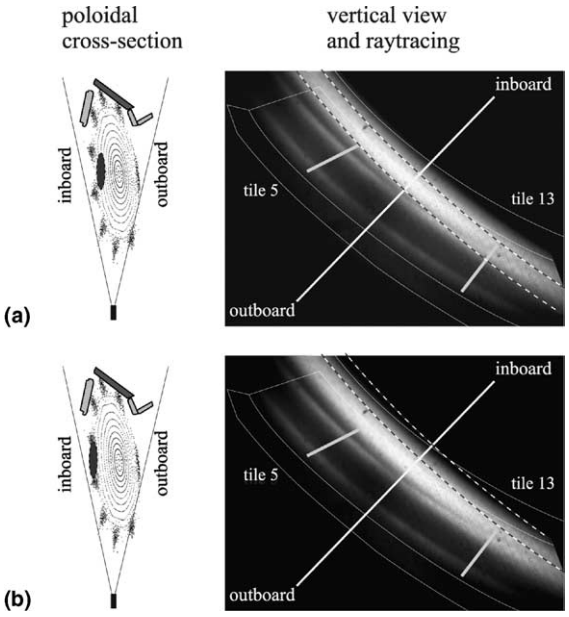

Fig. 6. Comparison of forward calculation and experimental results for W7-AS discharge #55521. The first column shows the magnetic flux surfaces from vacuum field calculations in the poloidal plane of the vertical camera. The assumed position of the model toroidal radiation belt is indicated by the filled ellipse ((a)-outside and (b) inside the main plasma). In the second column the position of the toroidal belt according to forward calculation (dashed lines show the boundary) and the divertor structure (solid lines) are indicated in the H_α image recorded by the vertical camera.

forward calculation method is used which is based on the calculated vacuum magnetic field and other model data. The basic idea is to project any geometric information (of field lines, divertors and baffles, etc.) into an image with the visual perspective according to the view and location of the camera mounted on W7-AS. It is found that the experimentally observed stripes oblique to the curvature of the divertors are compatible with a poloidal elongated radiation zone which extends in toroidal direction (without rotational transform) [11]. In Fig. 6, the projections for two different radial locations of such a toroidal belt are indicated in an experimentally observed image of a Marfe (discharge #55521). As the calculations show, the more inside the Marfe the more the inner strike line is covered. For the special shot #55521 for which the calculations were carried out we find a good agreement supposing a radial position of the toroidal belt just inside the last closed flux surface (LCFS), i.e. on closed flux surfaces. This finding supports the interpretation that the radiation belt is the result of a radiative condensation phenomenon. It was experimentally shown in the ALCATOR C-mod tokamak that the Marfe resides on closed flux surfaces [12]. Furthermore, the plasma in the center of the Marfe was recombining. Thus, it can be well detected by the H_α emission.

5. Summary

In the detached discharges of the W7-AS stellarator we observe a carbon radiation belt in the inboard SOL (and not in H_α). This phenomenon is explained by the EMC3-Eirene modeling as follows. At low divertor temperatures the carbon radiation moves away from the target plates (detachment process). It cannot stabilized within the divertor plasma but only in the inboard SOL in the region of the islands. The temperature in the divertor is still high enough to excite and ionize the hydrogen atoms there. Thus, the hydrogen emission dominates in the divertor but the carbon emission (CIII) in the inboard SOL. The modeling shows lower temperatures in the inboard SOL compared to the outboard SOL. Consequently, the region at the divertor target plates which is connected to the inboard side detaches at first. The region connected to the outboard side of the SOL stays attached (partial stable detachment) [3]. This kind of asymmetry is similar to the tokamak where a temperature asymmetry of the inner and outer divertor plasma was found [13].

At higher density we observe a belt of carbon and H_α radiation. The divertor plasma is completely detached under these conditions. Ray-tracing modeling shows that the H_α radiation resides on closed flux surfaces suggesting the formation of a Marfe similar to those in tokamaks (radiative condensation). The current free stellarator plasma does not collapse as a whole but the penetration of the radiation belt into the confinement region results in a confinement degradation and an unstable edge plasma as evident by the large H_α oscillations.

Thus, we consider this phase as the operational limit (density limit at about $4 \times 10^{20}\,m^{-3}$).

References

[1] K. Mccormick et al., Phys. Rev. Lett. 89 (2002) 015001.
[2] N. Ramasubramanian et al., Nucl. Fus. 44 (2004) 992.
[3] P. Grigull et al., Plasma Phys. Control. Fus. 43 (2001) A175.
[4] A. Loarte, J. Nucl. Mater. 241–243 (1997) 118.
[5] M. Greenwald, Nucl. Fus. 44 (2004) R27.
[6] L. Giannone et al., Plasma Phys. Control. Fus. 44 (2002) 2149.
[7] U. Wenzel et al., J. Nucl. Mater. 313–316 (2003) 1098.
[8] P. Grigull et al., J. Nucl. Mater. 313–316 (2003) 1287.
[9] Y. Feng et al., Plasma Phys. Control. Fus. 44 (2002) 611.
[10] U. Wenzel et al., Plasma Phys. Control. Fus. 44 (2002) L57.
[11] H. Thomsen et al., Nucl. Fus. 44 (2004) 820.
[12] B. Lipschultz et al., Phys. Rev. Lett. 81 (1998) 1007.
[13] U. Wenzel et al., Nucl. Fus. 41 (2001) 1695.